Trends in Peptide and Protein Sciences
Volume 5 (2020): e4

DOI: http://dx.doi.org/10.22037/tpps.v5i0.31578

Original Article

N-Succinyl-L,L-Diaminopimelic Acid Desuccinylase (DapE) a Potential Biomarker of *Mycobacterium Tuberculosis*: Tag-Free Purification by Metal Affinity Chromatography

Chinmay P. Umbarkar [a, b], Prashant S. Thakre[a], Supriya A. Kashikar[a], Niraj A. Ghanwate[b] and Vinod B. Agarkar [a*]

[a] *GeNext Genomics Pvt. Ltd., Nagpur, MS, India.*
[b] *Department of Microbiology, Sant Gadge Baba Amravati University, Amravati, MS, India.*

Article history:
Received: 3 August 2020
Accepted: 5 September 2020

Keywords:
Affinity chromatography
DapE
Mycobacterium tuberculosis
Protein

HIGHLIGHTS

- Expression and purification of recombinant Mtb-DapE$_{TagFree}$.
- On-column refolded protein with 98% purity from inclusion bodies purified by zinc-NTA column affinity chromatography.
- The purified protein observed no aggregation and degradation even after 8 months storage.
- ELISA and IFA results supports for development of detection assay for TB from tubercular samples.

ABSTRACT

DapE is an enzyme which is highly essential in lysine biosynthetic pathway for the growth and survival of *Mycobacterium tuberculosis* (*Mtb*) and other bacterial species although absent in human host. However, the sequence identity of *Mtb*-DapE with other mycobacterium and bacterial species estimated between 93 to 75% and approximately 50%, respectively. DapE is a metallo-enzyme requires few of transition metals for activity and bacterial proliferation. The homology model based structural studies including published structures revealed an availability of zinc interacting conserved amino residues in *Mtb*-DapE. In this study, we purified full length recombinant *Mtb*-DapE as tag-free (*Mtb*-DapE$_{TagFree}$) protein from inclusion bodies using zinc-NTA column. The single step purified protein observed with 96-98% purity and high yield. The indirect ELISA had 40% sensitivity using *Mtb*-DapE as an antigen against bovine tuberculosis (bTB) serum samples. IFA analysis with clear fluorescent spots of *Mtb* native DapE antigen in (3+) human TB positive sputum samples and recombinant *Mtb*-DapE positive control against *Mtb*-DapE polyclonal antibody are highly encouraging. The ELISA and IFA results incite for the consideration of *Mtb*-DapE in future development of quick and ideal TB detection assay along with other *mycobacterium* antigens. The future advanced detailed structural and functional studies using this highly purified and tag-free *Mtb*-DapE may provide discovery of antitubercular drug(s) and promising inhibitory molecules.

Introduction

Tuberculosis (TB) is an ancient communicable airborne disease causes by *Mycobacterium tuberculosis* (*Mtb*). The emergence of multidrug resistant (MDR) and extensively drug-resistant (XDR) strains has caused the increase in TB cases. However, 1.5 million people died in 2018 due to TB including who had lived with HIV infection. TB is preventable, treatable and curable (Vasantha and Venkatesan, 2014; Agins, et al., 2019).

C. P. Umbarkar: https://orcid.org/0000-0001-9416-1945
V. B. Agarkar: https://orcid.org/0000-0001-9906-5223
[*] *Corresponding Author:*
Email: vinodagarkar@gng.asia (V. B. Agarkar)

Years of study developed almost 20 antitubercular drugs. Recently, in 2019, U.S. Food and Drug Administration (US-FDA) approved the new drug Pretomanid in combination of Bedaquiline and Linezolid for treatment of TB (Maxmen, 2019). Nevertheless, tuberculosis is the global high risk issue for persons with compromised immune system, tobacco consumption, malnutrition and diabetic. World Health Organization (WHO) and several countries including India have targeted for the elimination of TB by year 2025-2030. Active TB person with mild symptoms delays in diagnosis and treatment, results in the transmission of infection to other close contacts. The early and rapid diagnosis, decreasing the duration of therapy, early treatment and prevention are the key factors for complete elimination of TB.

Succinyl-diaminopimelate desuccinylase (DapE) lysine biosynthesis pathway is necessary for the protein synthesis and formation of peptidoglycan cell wall in bacteria and plants. Lysine biosynthesis and DapE absent in human as lysine is an essential amino acid. Finding inhibitor for predominantly pathway inhibition of DapE would not destruct or be toxic for the human cell mechanism. Moreover, this strengthens and provide better idea for prediction and drug designing. The structural and functional amino acid conservation in bacterial DapE is significant. However L-captopril, L-penicillamine and 2-thiopheneboronic acid inhibits bacterial HiDapE and NmDapE while not substantial inhibition of *Mtb*-DapE (Gillner, et al., 2009; Uda and Creus, 2011; Greenfield and Harlow, 2014; Starus, et al., 2015).

Zinc binding properties are exploited for the purification of zinc finger domains and zinc proteinases by immobilized zinc affinity chromatography (Wilfong, et al., 2010; Voráčková, et al., 2011). Here, we expressed and purified stable well folded zinc binding *Mtb*-DapE$_{Tag\text{-}Free}$ protein from inclusion bodies with high yield using zinc-NTA metal affinity chromatography. The purified *Mtb*-DapE$_{TagFree}$ protein would be used for future structural and functional studies to open the platform for the prediction of better *Mtb*-DapE inhibitory molecule. Polyclonal antibody raised against *Mtb*-DapE$_{6XHIS}$ recognized the *Mtb*-DapE$_{TagFree}$. IFA and ELISA observations are proposing *Mtb*-DapE as the potential biomarker for TB diagnosis.

Materials and Methods

Materials

Restriction enzymes (New England Biolabs); Protein expression plasmids and *E. coli* strains (Novagen); Balb/c mice (National Institute of Nutrition, Hyderabad); Ni-nitrilotriacetic acid agarose (NTA) beads (Qiagen); Isopropyl β- d-1-thiogalactopyranoside (IPTG) (MP Biomedical); Luria-Bertani media (Amresco); Antibiotics (Hi-media); Buffer constituents and other chemicals (SIGMA and Hi-Media); Western Blot nitrocellulose paper (Pall Life Sciences); Protein A resin (GeneScript); CNBr-activated sepharose 4B column (GE Healthcare Life Sciences), TMB (Sigma), Goat ant-mouse HRPO conjugated antibody (Thermo Scientific).

Ethics statement

The handling of samples and immunofluorescence assay preparation was performed in biosafety level-3 (BSL-3) containment facility under the guidance of experts at Mahatma Gandhi Institute of Medical Science (MGIMS), Sewagram Hospital, Wardha (MS). TB infected (3+) positive and negative human sputum samples collected for assay were numerically coded by laboratory. The identity of persons not revealed to any researchers or persons except responsible clinicians. The included samples in this study were routinely collected samples for pathological diagnosis of TB.

Bioinformatics and homology model analysis

Mtb-DapE protein sequence retrieved from *Mtb*-DapE$_{HM28}$ plasmid sequencing results (Umbrakar et al., 2019) Nucleotide sequence converted in to amino acid and NCBI blast alignment resulted 100 % identity with 354 amino acids of DapE *Mycobacterium tuberculosis* H37Rv (Gene ID 887386 and protein accession YP_177796). The physico-chemical properties such as molecular weight, isoelectric point, atomic composition, extinction coefficient and hydropathicity were calculated using ExPASy-Protparam (Gasteiger et al., 2005). The secondary structure was predicted by SOPMA (Geourjon and Deleage, 1995). DISULFIND tool was used for disulfide bond predictions (Ceroni et al., 2006). Our previously published data (Umbarkar et al., 2019) of CD spectral analysis and protein sequence alignment predicted ArgE crystal structure (PDB ID 3tx8) as a best candidate for homology modeling. The predicted template was used for *Mtb*-DapE protein homology structure modeling using Easy Modeller 4.0 (Bhusann et al., 2010). The structural model was validated using ProSA, QMEAN and Verify 3D (Bowie et al., 1991; Lüthy et al., 1992; Wiederstein and Sippl, 2007; Studer et al., 2020). The created homology model was evaluated using Chimera 1.11.2 and Pymol (DeLano, 2002; Pettersen et al., 2004).

Construction of recombinant plasmid

The aforementioned *Mtb*-DapE$_{HM28}$ plasmid was used for construction of six histidine tag-free plasmid.

Briefly, PCR performed using *NdeI* and *XhoI* restriction sites inserted in forward 5'-ATTTACATATGGCTAGT GGACGCGGGGACCC-3' and reverse 5'-TATAAAT ACTCGAGTCAACCCAGGTATCGGCGCAGCAAGT CCAC-3' primers, respectively. Amplified gene product from *Mtb*-Dap_{EHM28} plasmid and pET21a vector was digested by *NdeI* and *XhoI* restriction enzymes, analyzed and purified on 1 % agarose gel electrophoresis. The resulted gene ligated in pET21a and transformed in chemically competent *E. coli* DH5α cells. The positive clones screened by gene specific primers and restriction digestions. The recombinant plasmid was named as *Mtb*-Dap_{ENH21}. The forward and reverse sequencing results confirmed the correct orientation and sequence.

Protein expression as in inclusion bodies

Mtb-$DapE_{NH21}$ plasmid was transformed in BL21 (DE3) competent cells. *Mtb*-$DapE_{NH21\BL21}$ cells grown in Luria-Bertani (LB) growth media supplemented with ampicillin (100 µg/ml). Overnight primary culture re-inoculated in ampicillin selected LB media shaking flasks at 220 rpm and allowed to grow for 3 hours at 37 °C. The culture was induced by 0.1 mM IPTG and harvested in next 3-4 hours. Harvested cells proceeded for sonication in extraction buffer 50 mM Tris-HCl pH 8.0, 300 mM NaCl, 10% glycerol, 10 mM βME, 1 mM EDTA and 1 mM PMSF. The supernatant discarded after 30 minutes centrifugation at 16000 rpm and remaining cell pellet (insoluble inclusion body form) was re-suspended in extraction buffer without EDTA containing 0.1 % Triton X-100. Re-suspended pellet was shaken at room temperature for 30-40 minutes and centrifuged at 16000 rpm for 20 minutes. Obtained cell pellet was washed 2-3 times with 500 mM NaCl in 50 mM Tris-HCl pH 8.0, buffer. Finally, inclusion bodies separated from suspension by centrifugation at 16000 rpm. *Mtb*-$DapE_{TagFree}$ inclusion bodies suspended by mixing with pipetting in buffer A containing 50 mM Tris-HCl pH 8.0, 300 mM NaCl, 20 % glycerol, 10 mM βME and 8 M Urea.

Preparation of cation metal NTA beads for protein binding assays

4 ml of Ni-NTA agarose resin packed in small column. High concentration of EDTA used for strip-off nickel from NTA (instruction manual of Qiagen). Nickel free NTA extensively washed with distilled water following with 50 mM Tris-HCl pH 8.0 buffer. One ml of washed NTA resin mixed with 1 ml of 0.1 % cationic metal salts of cobalt (II), zinc (II), cadmium (II) and nickel (II) chlorides, separately. Unbound metals washed off using Milli Q water and 50 mM Tris-HCl pH 8.0 buffer containing 10 mM imidazole, 300 mM NaCl and 20% glycerol. Prepared metal bound resins as Co-NTA, Zn-NTA, Cd-NTA and Ni-NTA used for protein metal binding assay.

Protein purification

The temperature 4 °C was maintained during all protein purification steps. The solubilized cell pellet comprising inclusion bodies centrifuged at 16000 rpm for 60 minutes to remove insoluble particulates. The clarified supernatant was allowed to bind cation metal-NTA resin pre-equilibrated with buffer A for overnight with continuous rotation. Protein bound resin packed in column and washed twice with buffer A. Three more washes with 0.1 ml/minute flow rate were applied using gradually decreasing concentration of 6 M, 4 M and 2 M urea containing buffer A. The column was extensively washed with buffer B containing 50 mM Tris-HCl pH 8.0, 300 mM NaCl, 20% glycerol, 10 mM βME, 2 M urea and 10 mM imidazole. The bound protein was eluted with buffer B containing 200 mM imidazole. Eluted fractions were subjected for overnight dialysis in buffer C containing 30 mM Tris-HCl pH 8.0, 112 mM NaCl, 1mM DTT and 10% glycerol. The same protocol was applied for Co-NTA, Zn-NTA, Cd-NTA and Ni-NTA columns for purification of *Mtb*-$DapE_{TagFree}$.

Size exclusion chromatography

The refolded *Mtb*-$DapE_{TagFree}$ protein centrifuged at 18000 rpm for 1 hour. Collected clarified protein solution subjected to increase NaCl concentration up to 300 mM and filtered through 0.22 µm membrane filter. Subsequently, as final polishing step, protein was loaded on to size exclusion chromatography column (Superdex S200 16/60 GE Healthcare) attached with AKTA purifier 100. The equilibration and elution buffer D containing 30 mM Tris-HCl pH 8.0, 300 mM NaCl and 1 mM DTT was used. Protein purity and molecular weight was analyzed on 12% SDS-PAGE. Protein quantification was performed by Bradford assay (Sigma).

Production of polyclonal antibody (pAb)

Previously purified *Mtb*-DapE 6XHIS tag full length protein (*Mtb*-$DapE_{6XHIS}$) was used as an antigen (Ag) for the production of pAbs (Umbarkar et al.,2019). Ag was mixed with Freund's adjuvant for enhancing immune response in Balb/c mice strain. Blood was collected for titer expansion through orbital sinus of mice after every booster to monitor the immunogenicity. Four boosters with 25 µg antigen concentration per mice at 14 days interval were executed. pAbs present in serum separated from coagulated blood were analyzed by indirect ELISA

(Cooper and Paterson, 2000; Greenfield and Harlow, 2014). ELISA was performed using 2 µg/ml *Mtb*-DapE (*Mtb*-$DapE_{6XHIS}$ or *Mtb*-$DapE_{TagFree}$) in 1X PBS buffer coated on polypropylene Maxisorp ELISA plate and incubated at 4 ºC, overnight. The blocking was done with 2% BSA and 1X PBST used for washing. A polyclonal serum with serial dilution ranging 1:300 to 1:72000 was used as primary Ab. Diluted goat anti-mouse HRPO conjugated Ab was used as the secondary Ab. 100 µl of tetramethylbenzidine (TMB) substrate was added for the enzymatic reaction and 0.2 N H_2SO_4 as reaction stop solution. Optical density was measured at 450 nm by spectrophotometer (Leenaars and Hendriksen, 2005). After fourth booster, 4 ml polyclonal serum was collected from 3 immunized mice. The purification of pAb was performed by 50% ammonium sulfate precipitation followed by Protein A resin or CNBr-activated sepharose 4B column according to the manufacturer's instructions. The purity of pAb was analyzed by 10% SDS-PAGE. The purified pAb titer was assessed using indirect ELISA similar to the serum ELISA described above.

Mtb-$DapE_{TagFree}$ protein confirmation by Western blotting

Western blotting was performed on 0.45 µm nitro cellulose membrane by standard procedures (Towbin et al., 1979). Briefly, *Mtb*-$DapE_{TagFree}$ electrophoretically transferred on membrane after 12% SDS-PAGE. The blocking was performed with 2% BSA in Tris buffer saline (TBS) overnight at 4 °C. Membrane was washed thrice with 1X TBS supplemented with 0.05% Tween-20. The aforementioned purified *Mtb*-$DapE_{6XHIS}$ pAb was used as the primary Ab and goat anti mouse HRPO conjugated Ab used as the secondary Ab. The blot was developed using TMB as a substrate.

Presence of Mtb-DapE specific antibody in bovine TB sample

The PCR analyzed total number of 28 confirmed positive and negative bTB serum samples from Government Veterinary Institute Nagpur (India) were collected. The indirect ELISA was performed for the detection of specific IgG from biological sample as above (Cooper and Paterson, 2000; Greenfield and Harlow, 2014). Briefly, recombinant *Mtb*-$DapE_{TagFree}$ protein coated at the 0.5 µg/ml concentration in Nunc maxisorp ELISA plate overnight at 4 °C and blocked with 2% BSA. The collected bTB serum sample added at 1:300 dilutions and incubated for 1 hour at 37 °C. Anti-Cattle HRPO conjugated antibody (Bethyl, A10-230P) was added and incubated for another 1 hour at 37 °C. Plate washed and color was developed using TMB substrate. 1X PBST was used for washing during each step. Optical density was measured at 450 nm using spectrophotometer.

Immunofluorescence assay (IFA) for detection of Mtb-DapE from sputum sample

Purified *Mtb*-$DapE_{6XHIS}$ pAb was used for detection of TB in human's sputum samples by IFA with few modifications (Cimino et al., 2006; Anindita et al., 2010; Singh et al., 2016). The collected TB infected (3+) positive and negative sputum samples were confirmed through Acid Fast staining and BACTEC™ MGIT™ 960 system at MGIMS, Wardha. *Mycobacterium Tuberculosis* H37Rv (ATCC no. 27294) and *E. coli* cultures were used as a positive and negative controls, simultaneously. *Mtb*-$DapE_{6XHIS}$ protein was used as a standard control. Glass slides cleaned and wiped with 70% ethanol before use and labeled, accordingly. Smear in 0.1% Triton X-100 and 1X PBS was prepared in circle marked area and fixed by air dry and gentle heating. 2% BSA was used for blocking and unbound material extensively washed by 1X PBST. 2 µg/ml *Mtb*-$DapE_{6XHIS}$ pAb as a primary Ab poured on smear fixed area carefully and all slides were kept at 37 ºC in dark for 1 hour. The unbound material was washed out with 1X PBST and air dried. Anti-mouse IgG FITC labeled Ab was used as a secondary antibody with dilution of 1:700 and all slides were kept at 37 ºC in dark for 1 hour incubation. All slides were washed properly to remove unbound antibodies. Cover slips were used with oil emulsion and immediately observed under FITC fluorescent microscope (Zeiss Axiovert 200M Inverted Fluorescence Microscope).

Results and Discussion

The utilization of tags (GST, HIS, MBT, NuSa, etc.) are popular for expression and purification of proteins. In our previous studies we successfully expressed and purified *Mtb*-$DapE_{6XHIS}$ inserting C-terminus six histidine tag with high yield from inclusion bodies (Umbarkar et al., 2019). However several publications provide evidences that the tags influence the structural and biophysical studies with negative impact on conformation, solubility and biological activity of the protein (Fonda, 2002; Chant et al., 2005). Here, we established the single step preparation of tag-free *Mtb*-DapE protein using zinc-NTA based metal affinity chromatography.

Bioinformatics, homology model and metal binding site identification

The primary structure of *Mtb*-$DapE_{TagFree}$ protein contains 354 amino acids. The protein sequence

percentage identities with DapE of other *mycobacterial* species were estimated between 93 to 75%. The theoretical molecular weight 37273 Da, pI 5.31, molar extinction coefficient 26930 M^{-1} cm^{-1} and total number of 34 positively and 45 negatively charged residues were estimated. No disulfide bonding was predicted. The secondary structure prediction identified 11 beta sheets and 11 alpha helices with three domain structure. However, it shares 55% sequence identity with *Corynebacterium glutamicum* ArgE crystal structure (PDB entry 3tx8) (Fig. 1).

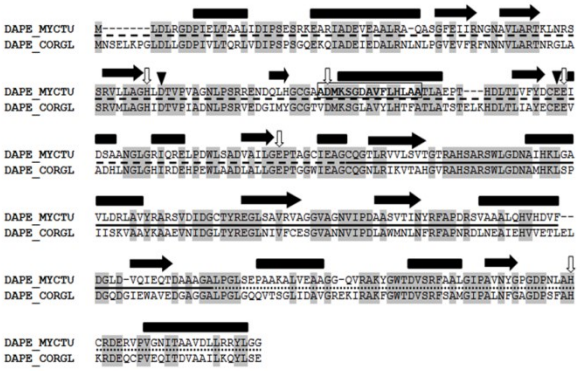

Figure 1. Amino acid sequence alignment of *M. tuberculosis* (MYCTU) with *Corynebacterium glutamicum* ArgE (CORGL). Domain 1 (AA 1-164_dash line), domain 2 (AA 165-277_solid line), domain 3 (78-354_dot line), helix (rectangle), sheet (right arrow), conserved residues (grey highlighted), residues involved in metal binding (down arrow), active site residues (inverted triangle), transmembrane helical amino acids stretch or membrane interaction (bold bracketed, MEMSAT prediction).

The transition metals play a key role in various biochemical processes including structural stabilization and catalytic activity of proteins. Several studies concluded the role of zinc binding proteins in microbial growth, development and pathogenesis. The high resolution X-ray crystal structures of *Haemophilus influenzae* DapE (PDB entries 3isz and 3ic1) reported with one and two zinc ions bound in the active site, respectively (Nocek et al., 2010). The crystal structures (PDB entries 4o23 and 4ppz) of mono and di-zinc DapE form of *Neisseria meningitides* MC58 with conformational change in catalytic domain rotation relative to dimerization domain as the consequences of dinuclear zinc(II) cluster were also reported (Starus et al., 2015; Boguslaw, 2018). Usha V *et al.* reported the *Mtb*-DapE lost the activity following chelating of zinc (Usha et al., 2016*)*. However the atomic coordinates of 3tx8 PDB template was used for the homology modeling structure prediction of *Mtb*-$DapE_{TagFree}$. The Z-score -8.1 by ProSA was convincing for the excellent quality model. QMEAN global score of 0.8 and Verify 3D value of 90.4% supported the ProSa validation. In the model structure, 5 amino acids (His 69, Asp 95, Glu 126, Glu 154 and His 330) were predicted with plausible junction with zinc or other metals at active site *(Fig. 2A and 2B).*

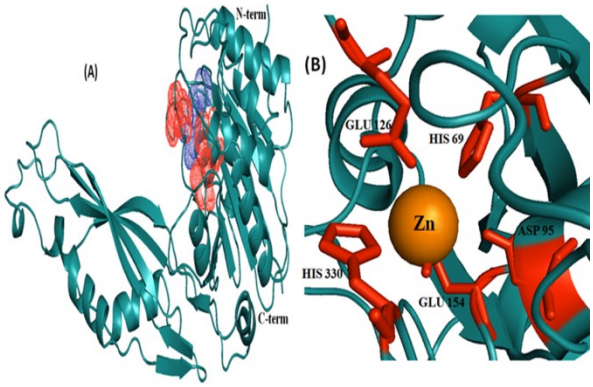

Figure 2. Cartoon representation of *Mtb*-$DapE_{TagFree}$ homology model structure. (A) Metal binding and active site region denoted in red and blue color dot surface respectively, (B) zinc II (yellow sphere) interacting amino acid residues shown as red sticks.

Recombinant plasmid preparation and protein expression

The preliminary X-ray diffraction analysis of *Mtb*-DapE published albeit crystal structure is missing where the majority of intergrown crystals with only few single crystals with no zinc in the active site were obtained (Reinhard et al., 2010). The purity of protein and C-6XHIS tag could be the concern as it may compete for zinc ion during purification. The aforementioned DapE homodimeric structures (PDB files) exhibits an active site junction between globular catalytic and dimerization domain. The model based structural studies including published structures revealed an availability of zinc interacting catalytic site conserved His 69, Asp 95, Glu 126, Glu 154 and His 330 amino residues in *Mtb*-DapE (Figure 2A and 2B). These studies influenced the purification of tag-free *Mtb*-DapE using the zinc charged column.

Mtb-$DapE_{M21}$ recombinant plasmid without 6XHIS tag was reconstructed from *Mtb*-$DapE_{HM28}$ (Umbarkar et al., 2019) using polymerase chain reaction inserting restriction enzyme sites, stop codon and re-cloning. The constructed plasmid was transformed into BL21 (DE3) cells. The only 1-2% of total protein obtained from protein expression was soluble, surprisingly. However, several attempts have made to increase the solubility even as decreasing the concentration of IPTG, change in growth medium and lowering the protein induction temperature up to 16 °C. Finally, over produced Mtb-$DapE_{TagFree}$ protein was found in inclusion bodies expressed at 37 °C.

Protein purification

During this study, we also purified *Mtb*-DapE$_{6XHIS}$ protein by Ni-NTA column similar to our previous report (Umbarkar et al., 2019) for polyclonal antibody preparation. The confirmation of *Mtb*-DapE$_{TagFree}$ protein in inclusion bodies increased the possibility of substantially obtaining large quantity of purified protein. Protein denatured in high molarity of urea containing buffer and binding performance was evaluated with Zn (II), Co (II), Ni (II) and Cd (II) bound NTA columns (Fig. 3 and Fig. 4).

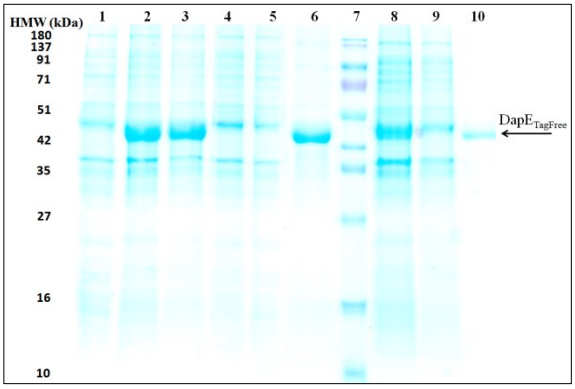

Figure 3. 12% SDS-PAGE analysis of DapE$_{TagFree}$ binding and elution by metal-NTA column. Lane 1: non-induced, lane 2: induced whole cells, lane 3: inclusion bodies in 8 M urea, lane 4: flow through of Zn-NTA column, lane 5: wash of Zn-NTA column, lane 6: elution of Zn-NTA column, lane 7: HMW, lane 8: flow through of Co-NTA column, lane 9: wash of Co-NTA column, lane 10: elution of Co-NTA column.

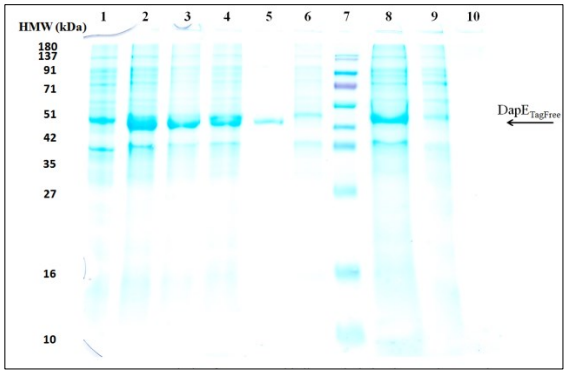

Figure 4. 12% SDS-PAGE analysis of DapE$_{TagFree}$ binding and elution by metal-NTA column. Lane 1: non-induced, lane 2: induced whole cells, lane 3: inclusion bodies in 8 M urea, lane 4: flow through of Ni-NTA column, lane 5: wash of Ni-NTA column, lane 6: elution of Ni-NTA column, lane 7: HMW, lane 8: flow through of Cd-NTA column, lane 9: wash of Cd-NTA column, lane 10: elution of Cd-NTA column.

The on-column refolding was performed with gradual decrease of urea concentration in final wash buffer. A large amount of unbound protein found in flow through of Co (II) and Ni (II) columns (Fig. 3 and Fig. 4). Cd (II) column was not shown any binding with protein (Fig. 4). More than 95% protein bound to the Zn (II) column and eluted with >95% purity (Fig. 5). The molecular weight of Zn-NTA column purified *Mtb*-DapE$_{TagFree}$ compared with Ni-NTA purified *Mtb*-DapE$_{6XHIS}$ protein using SDS-PAGE and there was no substantial difference observed in molecular weights between His tag and tag-free DapE (Fig. 6). The total of 20-22 mg protein was purified by Zn-NTA from one liter batch culture. However, finishing step of size exclusion chromatography lost 5-10% protein despite it yielded almost 98% purity (Fig. 7). The aliquoted protein stored in buffer containing 30 mM TrisHCl pH 8.0, 300 mM NaCl, 1 mM DTT and 2% glycerol at -80 °C and -20 °C was neither degraded nor aggregated as monitored for 8-10 months. The earlier reported yield of *Mtb*-DapE with 6 histidnine tag was 0.6-3 mg/liter culture pellet (Reinhard et al., 2010; Usha et al., 2016). Here, purified *Mtb*-DapE as highly stable, well folded, without tag, with high purity and high yield is an exceptional for any further studies including protein crystallization and structural studies.

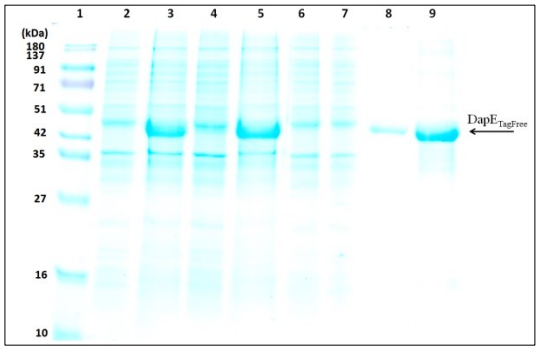

Figure 5. 12% SDS-PAGE analysis of DapE$_{TagFree}$ expression and purification by Zn-NTA column. lane 1: high molecular weight marker, lane 2: non-induced whole cells, lane 3: induced whole cells, lane 4: induced cells free extract, lane 5: inclusion bodies in 8 M urea, lane 6: flow through, lane 7: wash, lane 8: elution by 50 mM imidazole, lane 9: elution by 200 mM imidazole.

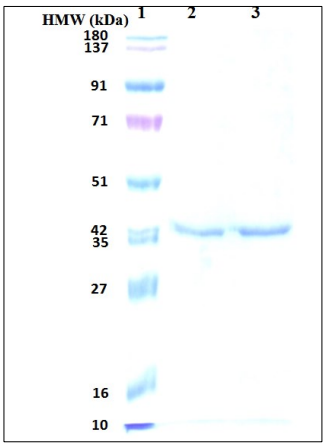

Figure 6. Molecular weight comparative analysis by 12% SDS-PAGE. Lane 1: HMW, lane 2: *Mtb*-DapE$_{6XHIS}$, lane 3: *Mtb*-DapE$_{TagFree}$.

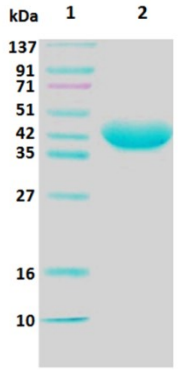

Figure 7. *Mtb*-DapE$_{TagFree}$ purified after Zn-NTA and size exclusion chromatography.

Western blotting, indirect ELISA and IFA

The preparation of *Mtb*-DapE$_{TagFree}$ was confirmed by western blotting using pAbs produced in mice against antigen *Mtb*-DapE$_{6XHIS}$ (Fig. 8). The indirect ELISA is usually advantageous due to simplicity predominantly while if basic access to purified and developed cost effective antigen production platform exist. Bovine TB PCR positive and negative serum samples were analyzed by indirect ELISA against *Mtb*-DapE$_{6XHIS}$. The secondary Anti-Cattle HRPO conjugated antibody detected the bovine serum Ab complexed with *Mtb*-DapE$_{6XHIS}$. Nine positive and six negative out of 28 PCR tested serum samples revealed incredibly convincing results. However, 13 PCR positive samples were found false negative at 0.4 OD (bracketed as of negative samples, Fig. 9). The indirect ELISA overall results were with just 40% sensitivity. However an immune response of cattle during the course of disease is the limitation because it is influenced by age, stress, weather irregular development of humoral immune response. The further implications in increasing sensitivity and specificity would require constructive and profound studies with few different bovine TB antigens.

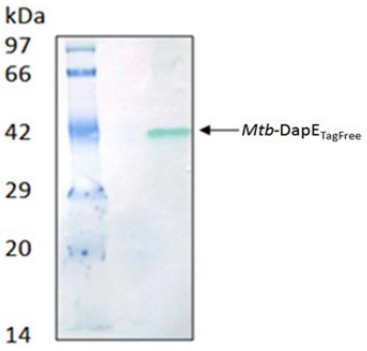

Figure 8. Western blot analysis of *Mtb*-DapE$_{TagFree}$ using polyclonal antibody raised against *Mtb*-DapE$_{6XHIS}$ protein.

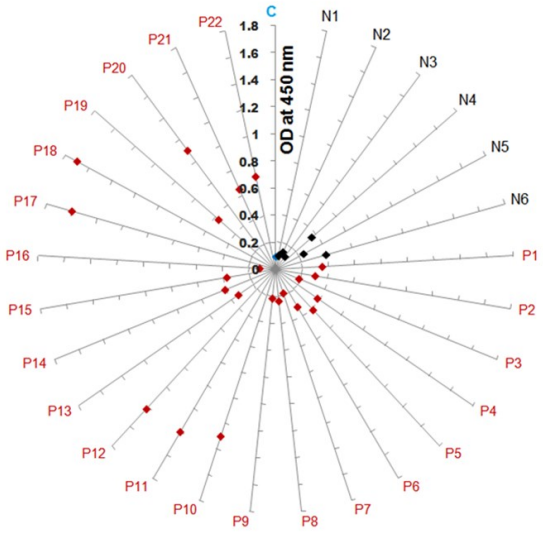

Figure 9. Indirect ELISA of bovine TB PCR positive and negative samples. C (cyan, no protein coated well), N (black, PCR negative), P (red, PCR positive).

The purified *Mtb*-DapE$_{6XHIS}$ Protein and pAb raised against same protein used in IFA. IFA of recombinant *Mtb*- DapE$_{6XHIS}$, *Mycobacterium tuberculosis* H37Rv pure culture and (3+) TB positive sputum samples were observed several fluorescent small, sharp and shiny dots (Fig. 10: A, B and C, simultaneously). However no analogous dots were seen in TB negative sample and *E. coli* pure culture (Fig. 10: D and E). IFA observations with clear fluorescent spots in smears of human TB positive samples and *Mtb*-DapE$_{6XHIS}$ protein as the positive control are highly encouraging for development of TB detection assay.

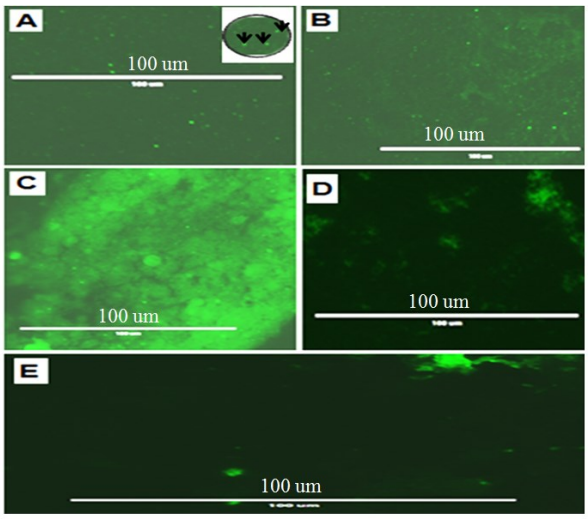

Figure 10. Immunofluorescence analysis. Shiny green dots as shown in arrow marked inset in Fig A indicate the DapE presence. (A) Recombinant *Mtb*-DapE, (B) *M. tuberculosis* H37 Rv culture, (C) TB positive sputum sample, (D) TB negative sputum sample, (E) *E. coli* culture.

Conclusion

The recombinant protein expression, purification and better yield with post purification stability are all time tough task. An expression and purification tags at either or both terminus of protein sequence provides some ease while purification and sometimes, makes challenges in the stability of proteins. Albeit for many studies including structural and molecular interactions, the tags become impediment. As far our understanding *Mtb*-DapE never expressed and purified without tag. Here, our combine results of *Mtb*-DapE$_{TagFree}$ single step purification without tag, indirect ELISA and IFA could benefit for structural and molecule based drug inhibitor studies. Furthermore production of poly and monoclonal antibodies against highly purified *Mtb*-DapE$_{TagFree}$ might impact on the development of quick and easy detection assay for TB from tubercular sputum samples.

Acknowledgements

The authors gratefully acknowledge the support and guidance of Dr. Rahul Narang, Department of Microbiology, Mahatma Gandhi Institute of Medical Sciences, Sevagram, India for IFA. We would also like to gratefully acknowledge the assistance of the research staff of Nagpur Veterinary College, Nagpur, India.

Competing Interests

The authors declared that there is no conflict of interest.

References

Agins, B. D., Ikeda, D. J., Reid, M. J. A., Goosby, E., Pai, M. and A. Cattamanchi, (2019). "Improving the cascade of global tuberculosis care: moving from the "what" to the "how" of quality improvement." *The Lancet Infectious Diseases*, **19**(12): 437-443.

Anindita, M., Thamke, D., Mendiratta, D. K. and B. C. Harinath, (2010). "Potential of Mycobacterial excretory secretory protein antigen (SEVA TB ES-31, ES-43, EST-6, ES-20) as a biomarker to detect Mycobacterium tuberculosis bacilli." *Indian Journal of Clinical Biochemistry,* **25**: 15-19.

Bhusan, K. K., Polamarasetty, A. and R. Pallu, (2010). "EasyModeller: A graphical interface to MODELLER." *BMC Research Notes*, **3**: 226.

Boguslaw, N. B., Reidl, C., Starus, A., Heath, T., Bienvenue, D., Osipiuk, J., Jedrzejczak, R., Joachimiak, A., Becker, D.P. and R.C. Holz, (2018). "Structural evidence of a major conformational change triggered by substrate binding in DapE enzymes: Impact on the catalytic mechanism." *Biochemistry*, **57** (5): 574–584.

Bowie, J.U., Lüthy, R. and D. A. Eisenberg, (1991). "Method to identify protein sequences that fold into a known three-dimensional structure." *Science*, **12**: 164-170.

Ceroni, A., Passerini, A., Vullo, A. and P. Frasconi, (2006). "DISULFIND: a disulfide bonding state and cysteine connectivity prediction server." *Nucleic Acids Research*, **34** (Web Server issue):177-181.

Chant A., Kraemer-Pecore C.M., Watkin R. and G. G. Kneale, (2005). "Attachment of a histidine tag to the minimal zinc finger protein of the *Aspergillus nidulans* gene regulatory protein AreA causes a conformational change at the DNA-binding site."*Protein Expression and Purification*, **39**(2): 152-159.

Cimino, M., Lorenzo, A. L. and L. Salazar, (2006). "Permeabilization of the mycobacterial envelope for protein cytolocalization studies by immunofluorescence microscopy." *BMC Microbiology*, **6**(35): 1-4.

Cooper, H. M. and Y. Paterson, (2000). "Determination of the specific antibody titer." *Current Protocols in Molecular Biology*, **50**(1): 11.17.1-11.17.13.

DeLano, W. L. (2002). "Pymol: An open-source molecular graphics tool." *CCP4 Newsletter on Protein Crystallography*, **40**: 82-92.

Fonda I., Kenig, M., Gaberc-Porekar, V., Pristovaek, P. and V. Menart, (2002). "Attachment of histidine tags to recombinant tumor necrosis factor-alpha drastically changes its properties." *Scientific World Journal*, **15**(2): 1312–1325.

Gasteiger E., Hoogland, C., Gattiker, A., Duvaud, S., Wilkins, M.R., Appel, R.D. and A. Bairoch, (2005). "Protein indentification and analysis tools on the ExPASy server." In John M. Walker (Ed), *The Proteomics Protocols Handbook,* Humana Press, pp. 571-607.

Geourjon, C. and G. Deleage, (1995). "SOPMA: Significant improvement in protein secondary structure prediction by c prediction from alignments and joint prediction." *CABIOS*, **11**: 681-684.

Gillner, D., Armoush, N., Holz, R. C. and D. P. Becker, (2009). "Inhibitors of bacterial N-succinyl-L,L-diaminopimelic acid desuccinylase (DapE) and demonstration of in vitro antimicrobial activity."*Bioorganic and Medicinal Chemistry Letters*, **19**(22): 6350–6352.

Greenfield, E. A. and E. Harlow, (2014). "Antibodies: a laboratory manual." In: E.A. Greenfield (Ed.), *Cold Spring Harbor, New York: Cold Spring Harbor Laboratory Press*.

Leenaars, M. and C. F. M. Hendriksen, (2005). "Critical steps in the production of polyclonal and monoclonal antibodies: evaluation and recommendations." *ILAR Journal*, **46** (3): 269-279.

Lüthy, R., Bowie, J.U. and D. Eisenberg, (1992). "Assessment of protein models with three-dimensional profiles." *Nature,* **356**(6364): 83-85.

Maxmen, A. (2019). "Treatment for extreme drug-resistant tuberculosis wins US government approval." *Nature*. News available at: https://www.nature.com/articles/d41586-019-02464-0.

Nocek, B. P., Gillner, D. M., Fan, Y., Holz, R.C. and A. Joachimiak, (2010). "Structural basis for catalysis by the mono- and dimetalated forms of the DapE-encoded N-succinyl-L,L-diaminopimelic acid desuccinylase." *Journal Molecular Biology*, **397**(3): 617-626.

Pettersen, E. F., Goddard, T.D., Huang, C.C., Couch, G. S., Greenblatt, D.M., Meng, E. C. and T. E. Ferrin, (2004). "UCSF Chimera--a visualization system for exploratory research and analysis." *Journal of Computational Chemistry*, **25**(13): 1605-1612.

Reinhard, L., Mueller-Dieckmann, J. and M. Weiss, (2012). "Cloning, expression, purification, crystallization and preliminary x-ray diffraction analysis of succinyl-diaminopimelate desuccinylase (Rv1202, DapE) from Mycobacterium tuberculosis." *Acta Crystallographica*, **F68**: 1089–1093.

Singh, S.V., Stephen, B.J., Singh, M., Gupta, S., Chaubey, K.K., Jayaraman, S., Sachan, T.K., Aseri, G.K., Dutta, M., Sohal, J.S., Dhama, K., Mukartal, S.Y. and R. Doddamane, (2016). "Evaluation of indirect fluorescent antibody test as a potential screening test for *Mycobacterium avium* subspecies paratuberculosis using milk of lactating domestic livestock." *Journal of Experimental Biology and Agricultural Sciences*, **5**: 533-540.

Starus, A., Nocek, B., Bennett, B., Larrabee, J. A., Shaw, D. L., Lee, W.S., Russo, M. T., Gillner, D.M., Grzyska, M.M. , Joachimiak, A. and R. C. Holz, (2015). "Inhibition of the DapE-encoded N-succinyl-L,L-diaminopimelic acid desuccinylase from *Neisseria meningitidis* by L-captopril." *Biochemistry*, **54**(31): 4834–4844.

Studer, G., Rempfer, C., Waterhouse, A.M., Gumienny, G., Haas, J., and T. Schwede, (2020). "QMEANDisCo - distance constraints applied on model quality estimation." *Bioinformatics,* **36**: 1765-1771.

Towbin, H., Staehelin, T., and J. Gordon, (1979). "Electrophoretic transfer of proteins from polyacrylamide gels to nitrocellulose sheets:

procedure and some applications." *Proceedings of the National Academy of Sciences USA*, **76**(9): 4350–4354.

Uda, N. and M. Creus, (2011). "Selectivity of inhibition of N-succinyl-L,L-diaminopimelic acid desuccinylase (DapE) in bacteria: DapE is not the target of L-captopril antimicrobial activity. "*Bioinorganic Chemistry and Applications*, **2011**(306465): 6 Pages.

Umbarkar, C.P., Thakre, P.S., Kashikar, S. A., Ghanwate, N.A. and V.B. Agarkar. (2019). "Cloning, expression, and refolding of N-succinyl- L,L-diaminopimelic acid desuccinylase (MTB-DapE) of Mycobacterium tuberculosis." *International Journal of Life Sciences Research,* **7**(3): 110-115.

Usha, V., Lloyd, A.J., Roper, D.I., Dowson, C.G., Kozlov G., Gehring, K., Chauhan, S., Imam, H. T., Blindauer, C.A. and G.S. Besra, (2016). "Reconstruction of diaminopimelic acid biosynthesis allows characterisation of *Mycobacterium tuberculosis* N-succinyl-L,L-diaminopimelic acid desuccinylase." *Scientific Reports,* **6** (23191): 1-10.

Vasantha, M. and P.Venkatesan, (2014). "Structural equation modeling of latent growth curves of weight gain among treated tuberculosis patients." *PLoS One*, **9**(3): e91152.

Voráčková, I., Suchanová, S., Ulbrich, P., Diehl, W. E. and T. Ruml, (2011). "Purification of proteins containing zinc finger domains using immobilized metal ion affinity chromatography." *Protein Expression and Purification*, **79**(1): 88–95.

Wiederstein and Sippl, (2007). "ProSA-web: interactive web service for the recognition of errors in three-dimensional structures of proteins." *Nucleic Acids Research*, **35**: W407-W410.

Wilfong, E. M., Locklear, U. and E. J. Toone, (2010). "A single step purification for autolytic zinc proteinases." *Bioorganic and Medicinal Chemistry Letters*. **20**(1): 280–282.